

## LETTER TO THE EDITOR

### Controlling transient chaos

Tamás Tél†

Institute for Theoretical Physics, RWTH, D-5100 Aachen, and Institut für Festkörperphysik, Research Center Jülich, D-5170 Jülich, Federal Republic of Germany

Received 27 August 1991

**Abstract.** The method of Ott, Grebogi and Yorke is extended to control transient chaos. The controlled signal then exhibits a periodic behaviour which is qualitatively different from that of the actual attractor. The time needed to achieve control is shown to be constant and to lie in the order of magnitude of the transient lifetime. The number of controlled trajectories, however, decreases the maximum perturbation according to a power law. Applicability to experimental situations and comparison with permanent chaotic cases are discussed.

The problem of controlling chaos has attracted recent interest [1-11]. The method of Ott, Grebogi and Yorke (OGY) [3] has the unique feature that it enables one to select a *predetermined* time-periodic behaviour by making only *small* time-dependent perturbations. They show that permanent chaos can always be depressed by stabilizing one of the many unstable periodic orbits embedded in the chaotic attractor. The idea is to start with any initial condition, wait until the trajectory falls into a target region around the desired periodic orbit and then apply feedback control.

In this letter we demonstrate that transient chaos can also be controlled in the same spirit. This has the striking consequence that in such cases a behaviour completely *different* from that of the actual attractor(s) can be selected. Furthermore, the controlling process exhibits *novel* features: the time needed to achieve control turns out to be constant, independent of the maximum perturbation, as a consequence of the finite chaotic lifetime in the unperturbed system; the number of trajectories controlled does, however, depend on the maximum perturbation and follows a power law.

In systems exhibiting transient chaos there exists in phase space an invariant set called a *chaotic saddle* or *repeller* [12-15], together with an attractor which is often simple, i.e. periodic. Trajectories start from randomly chosen initial points then approach the attractor with probability one. Before reaching it, however, they might come close to the strange repeller and stay in its vicinity for a shorter or longer time. This results in the appearance of chaotic motion with an average lifetime of  $1/\kappa$  where  $\kappa$  is the *escape rate*, a basic characteristic of the chaotic repeller. Furthermore, the strange set has a fractal structure along both stable and unstable directions and, just like a chaotic attractor, appears to be the closure of an infinity of hyperbolic periodic orbits [16-18]. As an example, figure 1 shows the invariant sets (attractor and chaotic repeller) for the Hénon map  $x_{n+1} = a - x_n^2 + by_n$ ,  $y_{n+1} = x_n$  at a parameter setting where

† Address after 1 September 1991: Institute for Theoretical Physics, Eötvös University, Puskin u. 5-7, H-1088 Budapest, Hungary.

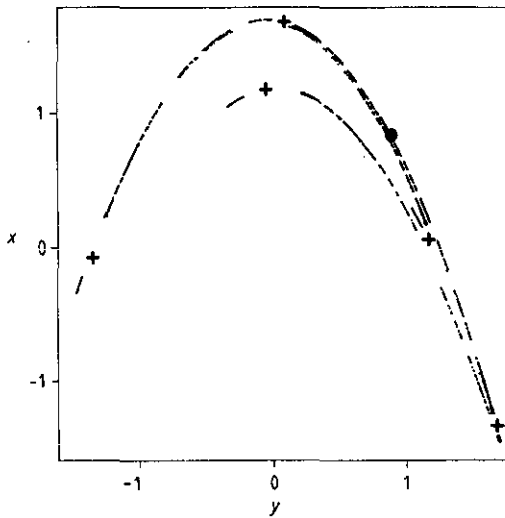


Figure 1. Invariant sets of the Hénon map  $x_{n+1} = a - x_n^2 + by_n$ ,  $y_{n+1} = x_n$  at the parameter setting  $a = 1.45$ ,  $b = 0.2$  where the attractor is a 5-cycle (black crosses). The fractal set is the chaotic repeller. Any periodic orbit on it can be stabilized by applying the method of OGY. We select the fixed point denoted by a dot.

the attractor is a period-5 orbit. Methods for constructing chaotic repellers are available [13–15]. Long-lived chaotic transients—the best candidates for experimental observability—are present around crisis configurations [12], at parameter values just beyond the disappearance of the chaotic attractor. It is worth mentioning that systems with fractal basin boundaries [19] are also accompanied by transient chaos since such boundaries are, in general, the stable manifolds of chaotic saddles.

The astonishing feature in controlling transient chaos is that one stabilizes an *atypical* behaviour associated with a chaotic repeller, a set with a measure zero basin of attraction. In order to achieve this, one has to use a large *ensemble* of points starting from some region of phase space including the repeller and concentrate on long-lived chaotic transients. We assume that the dynamics can be represented by a  $k$ -dimensional ( $k \geq 1$ ) nonlinear map  $\xi_{n+1} = f(\xi_n, p)$  where  $p$  is some accessible system parameter. We choose to stabilize a periodic orbit on the chaotic repeller and specify a target region around it. For simplicity, we take here always a fixed point but note that any of the hyperbolic periodic orbits of the strange set can be chosen, providing the method with a high degree of flexibility. Without loss of generality we set  $\xi = 0$  and  $p = 0$  at the desired fixed point.

Next, take a ball around the repeller (or some part of it), choose randomly a large number of points in it, and iterate them forward. Some will stay around the repeller over many time steps and might fall near the desired fixed point at  $\xi = 0$ . Therefore, wait until  $\xi_n$  of any trajectory enters the target region around the origin and then change the actual value  $p_n$  of the perturbation parameter  $p$  to be different from zero. Pick  $p_n$  so that the next iterate  $\xi_{n+1} = f(\xi_n, p_n)$  falls on the stable manifold of the origin of the uncontrolled map. If this is the case, the parameter perturbation can again be set to zero ( $p_{n+1} = 0$ ) and the orbit will approach the fixed point according to a geometric progression. This mechanism is exactly the same as for chaotic attractors; therefore, the result for the appropriate choice of  $p_n$  can be taken over from OGY. The computation based on the *linearized* dynamics around a fixed point of a two-dimensional map says

[3] that

$$p_n = \frac{\lambda_u}{\lambda_u - 1} \frac{\xi_n f_u}{g f_u}. \quad (1)$$

Here  $\lambda_u$  and  $f_u$  are the unstable eigenvalue of the fixed point in the uncontrolled map ( $p = 0$ ) and the corresponding left eigenvector, respectively. The quantity  $gp$  yields the shift of the position of the fixed point when changing the perturbation parameter by a small amount of  $p$ . It is supposed that the parameter  $p$  can be varied in a small range  $|p| < p_*$  only. Thus, if  $|p_n|$  happens to be greater than the maximum perturbation  $p_*$  we set  $p_n = 0$ . This last condition also specifies the size of the target where control is activated.

Using this algorithm the control of chaotic transients can be carried out. Figure 2 exhibits an uncontrolled transient chaotic signal of the Hénon map with a period-5 attractor, and its controlled version obtained by applying rule (1) with  $p_* = 0.1$ . This illustrates, by modifying a statement of OGY, that improvement is possible via small control even in systems with periodic attractors, provided they coexist with chaotic repellers in phase space. If the only invariant set is a periodic attractor, small perturbation can change the orbit only slightly [3]. If, however, weak chaos is present, i.e. the topological entropy of the system is positive, one can choose to stabilize any of the periodic orbits of the chaotic repeller. This leads to a behaviour, selected according to some criterion [3], which is completely different from that of the attractor.

The average time  $\tau$  needed to achieve control of permanent chaos was found [3] to depend on the maximum perturbation  $p_*$  according to a power law:  $\tau \sim p_*^{-\gamma}$  with an exponent  $\gamma \geq 1$  for small  $p_*$ . Here we show that this rule is no longer valid for transient chaos. The reason is that not all trajectories will now be controlled since the majority escapes the repeller before reaching the desired fixed point.

This can be best demonstrated by the example of one-dimensional maps. We consider a single humped map  $f(x)$  defined on some support interval and having a maximum outside this interval (see figure 3). Such maps generate transient chaotic signals and possess Cantor-like sets as their invariant repellers. The position of the actual attractor depends on the form of  $f(x)$  outside the support interval. Since it does not play any role in what follows, we do not specify this form. Let us start with a large number  $N_0$  of initial points distributed uniformly on the support. Control sets in if, after any number of iterations, a trajectory falls into the target region, an interval  $I$  of length  $\Delta$  around the fixed point  $x_F (\neq 0)$ . In general,  $\Delta$  is proportional to the maximum perturbation  $p_*$ . A single humped map  $f(x)$  can be embedded in two dimensions by considering the recursions  $x_{n+1} = f(x_n)$ ,  $y_{n+1} = x_n$ . The vectors  $f_u$  and  $g$  then point along the  $x$ -axis and the diagonal, respectively, and (1) can be applied. (In the example of the controlled parabola map  $x_{n+1} = a + p_n - x_n^2$ , (1) yields  $p_n = 2x_F(x_n - x_F)$  if  $|p_n| < p_*$ , and thus  $\Delta = p_*/x_F$ .) The number of trajectories controlled in the first step is proportional to the lengths  $\Delta_1$  and  $\Delta_0$  of the two pre-images  $I_1$  and  $I_0$  of the interval  $I$ , respectively, as shown in figure 3. One of the pre-images of the interval  $I_0$ , which contains the fixed point, falls into itself, the other one into  $I_1$ . Therefore, when counting the number of controlled trajectories in later steps, it is sufficient to follow the pre-images of  $I_1$  without those of  $I_0$ . The number of trajectories controlled in the  $n$ th step is thus proportional to the sum of the lengths  $l_i^{(n-1)}$ ,  $i = 1, 2, \dots, 2^{n-1}$  of the  $(n-1)$ th pre-images of  $I_1$ . Note that in transient chaotic cases these pre-images do not overlap for sufficiently small  $\Delta$ -values, i.e. for the maximum perturbation  $p_*$  much less than unity. The independence of the controlling time on  $p_*$  for  $p_* \rightarrow 0$  relies essentially on this property.

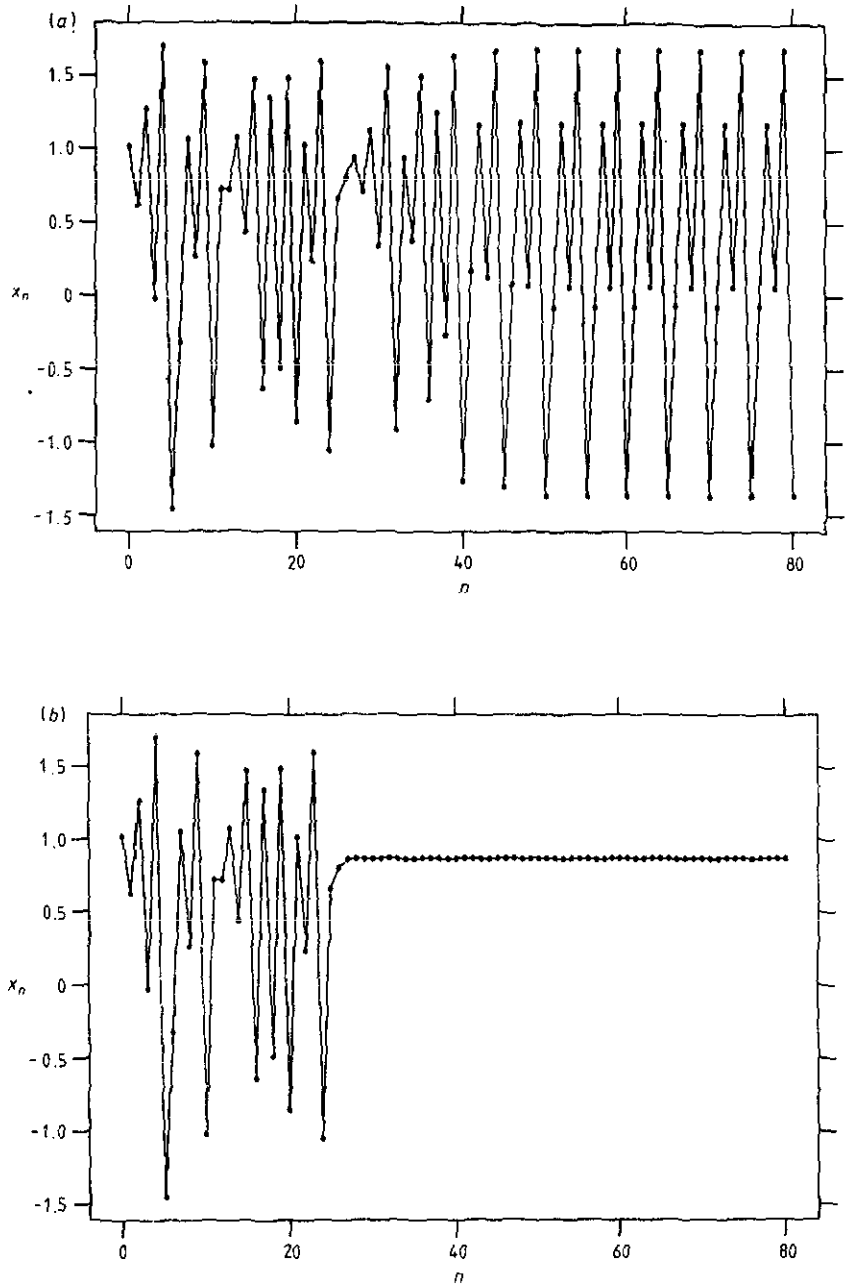
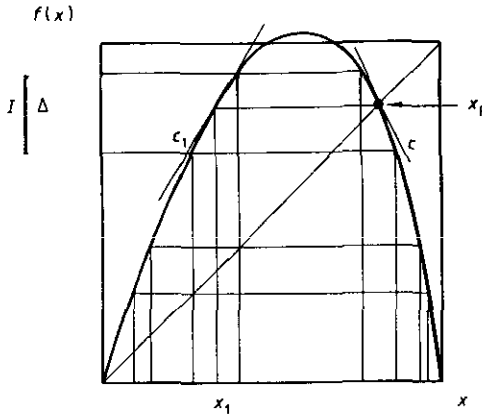


**Figure 2.** (a) Transient chaotic signal  $x_n$  versus  $n$  starting from the point  $x_0 = y_0 = 1.014782$  in the Hénon map of figure 1. The trajectory ceases to be chaotic at about the 38th time step where it comes to the neighbourhood of the attractor. (The average lifetime of chaotic transients is  $1/\kappa = 22$  at these parameters [13].) (b) Controlled signal started from the same initial point. The Hénon map was taken in the form given in the text with  $a = 1.45 + p_n$  where the perturbation parameter  $p_n$  is specified by (1) with  $p_* = 0.1$ . The fixed point is at  $x_F = y_F = 0.868858$ , and  $\mathbf{z}_n = (x_n - x_F, y_n - y_F)$ . Control sets in at the 26th step and the fixed point becomes stabilized.



$$\begin{aligned} \overline{I_1} & \qquad \overline{I_0} \\ \Delta_1 = \frac{\Delta}{c_1} & \qquad \Delta_0 = \frac{\Delta}{|c|} \end{aligned}$$

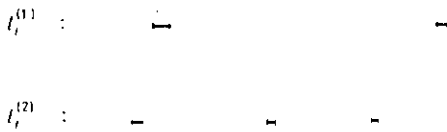


**Figure 3.** One-dimensional map generating transient chaos. Control is achieved if a trajectory falls into interval  $I$  having length  $\Delta$ . Some pre-images of  $I$  and their sizes relevant for computing the average time of control are also shown.

The total number of trajectories controlled at any time step can thus be expressed as

$$N = N_0 \left( \Delta_0 + \Delta_1 + \sum_{n>1} \sum_{i=1}^{2^{n-1}} I_i^{(n-1)} \right). \tag{2}$$

The total number of steps before control is then

$$T = N_0 \left( \Delta_1 + \sum_{n>1} \sum_{i=1}^{2^{n-1}} n I_i^{(n-1)} \right) \tag{3}$$

from which the average time to achieve control is computed as  $\tau = T/N$ . Next, let us observe that  $\Delta_0$  and  $\Delta_1$  can be obtained by dividing  $\Delta$  with the slopes  $c$  and  $c_1$  of the map taken at the fixed point  $x_F$  and its pre-image  $x_1$  (figure 3), respectively, for  $\Delta$  sufficiently small. In general, the length scales  $\{I_i^{(n)}, i = 1, \dots, 2^n\}$  can similarly be expressed by means of the derivative of the  $n$ -fold iterated map  $f^n$  taken at the  $n$ th pre-images of  $x_1$ . It has been shown [20] that the sum  $\sum_1^{2^n} |f^n'(f^{-n}(x))|^{-1}$  scales for large  $n$  at any value of  $x$  as  $\exp(-\kappa n)$  where  $\kappa$  is the escape rate. Therefore, the number of controlled trajectories can be rewritten for  $\Delta \rightarrow 0$  as

$$\begin{aligned} N &= N_0 \Delta \left( A + \frac{b}{c_1} \sum_{n=1}^{\infty} \exp[-\kappa(n-1)] \right) \\ &= N_0 \Delta \left( A + \frac{B}{c_1} \frac{1}{1 - \exp(-\kappa)} \right) \end{aligned} \tag{4}$$

with  $A$  and  $B$  as constants, because the sum converges for  $\kappa > 0$ . Similarly, we obtain

$$T = N_0 \Delta \left( C + \frac{B}{c_1} \frac{1}{[1 - \exp(-\kappa)]^2} \right) \quad (5)$$

where  $C$  is another constant. Since both  $N$  and  $T$  are now proportional to  $\Delta$ , the average time  $\tau$  to achieve control turns out to be independent of  $\Delta$  and, therefore, of the maximum perturbation  $p_*$ . For long-lived chaotic transients, i.e. for  $\kappa \ll 1$ , we find from (4) and (5) that  $\tau \approx 1/\kappa$ , which says that the time of control and the chaotic lifetime then coincide for  $p_* \rightarrow 0$ .

The argument breaks down at  $\kappa = 0$  since the geometric series does not converge and the pre-image intervals overlap, so that all trajectories will be controlled. Therefore, one expects for  $\kappa \rightarrow 0$  a crossover to the permanent chaos rule [3]  $\tau(\kappa = 0) \sim 1/p_*$  of one-dimensional maps if  $p_*$  is not infinitesimally small. Interestingly, the crossover can be seen in an extremely close neighbourhood of the crisis configuration only. To illustrate this, figure 4 shows  $\tau$  as a function of  $p_*$  for the parabola map at  $a = 2 + 10^{-6}$ . The behaviour can be understood by applying the following argument for  $\kappa$  and  $p_*$  small. Both the decay from the repeller and the decay into the target region are essentially random processes. In cases when the pre-images of the target region overlap, the rate constant of the control is essentially the same as that of permanent chaos, i.e.  $1/\tau(\kappa = 0)$ . These decay processes are, in a first approximation, independent, therefore, the combined process is described by the sum of the rates, and thus  $1/\tau = \kappa + 1/\tau(\kappa = 0)$ .

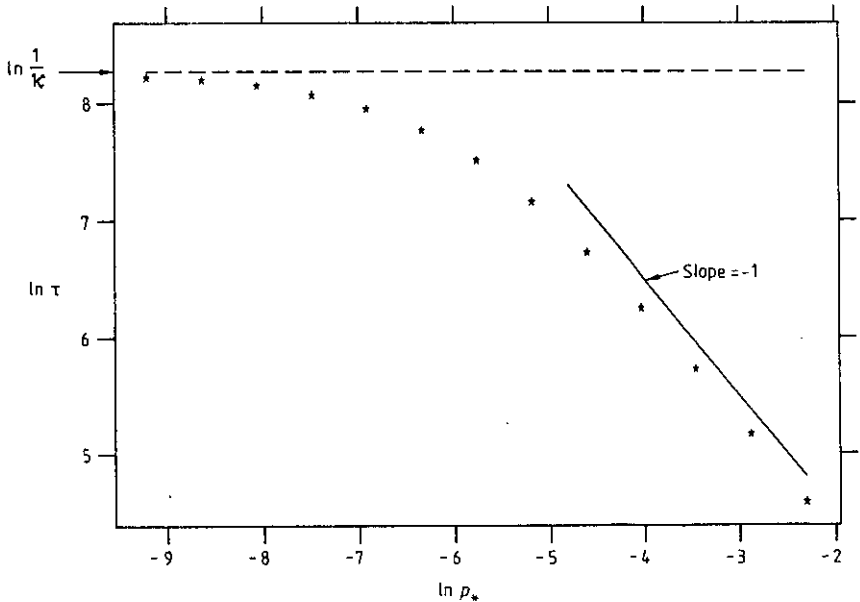


**Figure 4.** Average time  $\tau$  to achieve control versus the maximum perturbation in the parabola map  $x_{n+1} = a - x_n^2$  with  $a = 2 + 10^{-6}$ .  $10^5$  initial points uniformly distributed on the support were iterated either up to  $10^8$  steps or until they did not reach the interval  $I$  of length  $p_*/x_F$  around the fixed point  $x_F = 1 + 10^{-6}/3$ . The logarithm of  $\tau$  is plotted against  $\ln p_*$  in the range  $10^{-4} \leq p_* \leq 10^{-1}$ . The straight line shown has a slope  $-1$  and corresponds to the scaling in permanent chaos. Note the cross over into saturation for  $p_* < 10^{-3}$ . The broken line represents the average lifetime of transient chaos  $1/\kappa = 392.0$  in the uncontrolled system. The cross over into saturation cannot be seen any longer if  $a > 2 + 10^{-4}$ .

For one-dimensional maps  $1/\tau(\kappa=0) = cp_*$  where  $c$  is a constant, and we obtain  $\tau = 1/(\kappa + cp_*)$ , which gives a very good fit to the data of figure 4 with  $c = 0.0973$ . This rule also implies that the saturation range where  $\tau = 1/\kappa$  holds is reached for  $p_*$  smaller than some crossover value which scales with parameter  $a$  in the same way as the escape rate, i.e. as  $(a-2)^{1/2}$ .

The essential features in determining  $\tau$  were the following: (i) the pre-images of the fixed point's surrounding did not overlap, (ii) their characteristic lengths along the unstable direction could be summed up, yielding an exponential dependence on the escape rate, and (iii) the infinite sum of such factors was converging. Since these properties also hold for repellers of any higher-dimensional map, the time of control  $\tau(p_*)$  at a maximum perturbation  $p_*$  is expected to be found in general as

$$\tau(p_*) = \text{constant} \leq \frac{1}{\kappa}. \quad (6)$$

for  $p_*$  sufficiently small. Results for  $\tau$  of the Hénon map at the period-5 attractor are shown in the lower part of figure 5. The independence on the maximum perturbation is clear.

The number  $N(p_*)$  of the trajectories controlled is influenced by the shape and size of the region where control is activated. For two-dimensional maps, this is typically a parallelogram situated around the fixed point having some lengths  $l_1(p_*)$  and  $l_2(p_*)$  along the unstable and stable manifolds of this orbit, respectively.  $N(p_*)$  is obviously proportional to the probability of falling into the control parallelogram. Since we use an ensemble of trajectories distributed uniformly on a neighbourhood of the repeller, subsequent images of this neighbourhood will tend towards the unstable manifold of the chaotic set and the limiting distribution will be *smooth* on the manifold. The measure generated in this way is proportional to the so-called conditionally invariant measure [21, 18] (c-measure for short). Another relevant measure is the natural measure [13, 15, 18] obtained by taking the normalized restriction of the c-measure to the repeller, which is therefore not smooth along the unstable direction. The fractal properties of these measures along the stable manifold are, however, identical.

The c-measure of the control parallelogram can thus be written as

$$\mu(p_*) \sim l_1(p_*)l_2(p_*)^{\alpha_2} \quad (7)$$

with  $\alpha_2$  being the crowding index (pointwise dimension) along the stable direction at the hyperbolic fixed point of the repeller. Because of smoothness,  $\alpha_1 = 1$ . The non-trivial crowding index has been determined by means of the periodic orbit theory of strange sets and reads [18]

$$\alpha_2 = \frac{\ln|\lambda_u| - \kappa}{\ln 1/|\lambda_s|} \quad (8)$$

where  $\lambda_u(\lambda_s)$  denotes the larger (smaller) eigenvalue at the fixed point. Since for  $p_* \rightarrow 0$  the dimensions of the control parallelogram should be proportional to some powers of  $p_*$ , we find the number of controlled trajectories to follow a power law

$$N(p_*) \sim p_*^{\gamma(\kappa)} \quad (9)$$

with an exponent also depending on, besides local properties, the escape rate of the repeller. Although derived for maps of the plane, this law is conjectured to hold for higher dimensional systems, too.

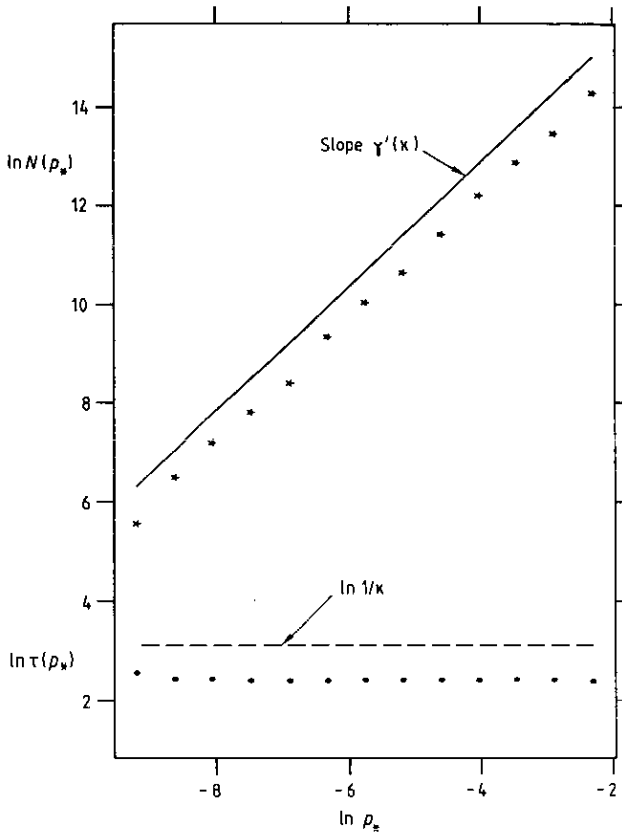


**Figure 5.** Average time to achieve control and number of controlled trajectories in the Hénon map with a period-5 attractor. Parameters as in figures 1 and 2.  $10^8$  initial points were distributed on the square ( $0 < x < 1$ ,  $-1 < y < 0$ ). Control was not activated during the first 10 steps. The number of further iterates of the non-escaping trajectories was computed until they did not fall within a circle around the fixed point with radius  $2.9p_*$ , in the range  $10^{-4} \leq p_* \leq 10^{-1}$ . Lower part: the logarithm of the average of these times as a function of  $\ln p_*$ . The broken line corresponds to the chaotic lifetime  $1/\kappa = 22$ . Upper part: the logarithm of  $N(p_*)$  against  $\ln p_*$ . The straight line has the slope  $\gamma'(\kappa) = 1.256$  given by (12). The results do not depend on the shape of the region where trajectories start from.

The control parallelogram mainly used by OGY has sizes proportional to  $p_*$  and  $p_*^{1/2}$  along the unstable and stable directions, respectively. With the same choice of the control parallelogram one thus finds the exponent for transient chaos to be

$$\gamma(\kappa) = 1 + \frac{1}{2} \frac{\ln|\lambda_u| - \kappa}{\ln 1/|\lambda_s|}. \quad (10)$$

Another way of specifying the condition for turning on the control is to take a ball of radius proportional to  $p_*$ . The corresponding exponent is then

$$\gamma'(\kappa) = 1 + \frac{\ln|\lambda_u| - \kappa}{\ln 1/|\lambda_s|}. \quad (11)$$

For one-dimensional maps  $\lambda_s = 0$  and  $\gamma(\kappa) = 1$  follows in agreement with (4).

In order to check the prediction, we initiated an ensemble of trajectories around the repeller of figure 1. They were first iterated up to 10 steps in order to have time

to approach the distribution corresponding to the c-measure. It was then determined how many trajectories fall in later steps into a circle of radius proportional to  $p_*$  centred at the fixed point, where iteration was stopped. (For the analogous permanent chaos case see [3].) The upper part of figure 5 shows  $\ln N(p_*)$  obtained this way against  $\ln p_*$ , along with the predicted slope.

At this point a simple argument can be given from which the difference between the control of permanent and transient chaos clearly follows. The number of trajectories controlled per time steps is proportional to the c-measure (natural measure in the permanent case)  $\mu(p_*)$  of the control parallelogram. The number  $N(p_*)$  of all controlled trajectories can then be estimated—up to a constant factor—as the measure multiplied by the number of iterates  $\tau(p_*)$  needed to achieve control in average. Therefore,

$$N(p_*) \sim \mu(p_*)\tau(p_*) \quad (12)$$

is expected to be valid for both permanent and transient chaos. For chaotic attractors all trajectories are controlled,  $N(p_*) = \text{constant}$ ; therefore,  $\tau(p_*) \sim 1/\mu(p_*)$  and the rule  $\tau(p_*) \sim p_*^{-\gamma(0)}$  derived by OGY is recovered. For transient chaos not extremely close to crisis we saw, on the contrary, that  $\tau(p_*) = \text{constant}$ , from which  $N(p_*) \sim \mu(p_*)$  follows.

Note that (12) seems to hold even if neither  $N$  nor  $\tau$  is constant. One can easily check that in the parabola map at  $a = 2 + 10^{-6}$   $N$  first grows linearly with the maximum perturbation but then (for  $p_* > 10^{-3}$ ) goes into saturation. Nevertheless,  $N(p_*)/\tau(p_*)$  is proportional to  $p_*$  in the *entire* range investigated.

In conclusion, we can see that controlling transient chaos is more difficult than permanent chaos as one has to use ensembles of trajectories, but it is also simpler since the time needed does not grow with decreasing perturbation and remains bounded by the average transient lifetime.

The assumption concerning the existence of a nonlinear map allows the investigation of any system, including experiments, for which a faithful Poincaré section can be constructed. Ensembles of trajectories can be generated by repeating the experiment several times with different initial conditions. Both the construction and the analysis of periodic orbits is nowadays straightforward [25] from measured time series. Unfortunately, the experimental investigation of transient chaos has received disproportionately little attention. Experimental control of permanent chaos has, however, been carried out [6–8] exactly in those systems (a driven magnetoelastic ribbon [22], a convection loop [23] and a spin wave [24] experiment) which had earlier been studied (at other parameter values, of course) in detail from the transient chaotic point of view. All these dynamics can be approximated by low-dimensional maps. Thus, we can hope that the possibility of stabilizing a non-trivial state in the presence of simple periodic attractors can be verified experimentally in these systems.

Finally, we mention that the results also hold in the Hamiltonian limit of transient chaos, which corresponds to chaotic scattering [26]. The method described here, together with the construction of the chaotic repeller, then provides us with the ability to stabilize intermediate complexes of driven classical scattering systems (e.g. chemical reactions) in time-periodic states.

The author is indebted to M Eisele, C Grebogi, Z Kovács and K G Szabó for useful comments and a critical reading of the manuscript. He thanks the referee for pointing out that the crossover process can be described by the sum of two decay rates. The

kind hospitality at the IFF of the KFA Jülich and at the Institute of Theoretical Physics of the RWTH Aachen is acknowledged.

## References

- [1] Fowler T B 1989 *IEEE Trans. Autom. Control* **34** 201
- [2] Hübler A and Lüscher E 1989 *Naturwissenschaften* **76** 67  
Hübler A 1989 *Helv. Phys. Acta* **62** 343  
Plapp B B and Hüber A 1990 *Phys. Rev. Lett.* **65** 2302  
Jackson E A 1991 *Physica* **50D** 341
- [3] Ott E, Grebogi C and Yorke J A 1990 *Phys. Rev. Lett.* **64** 1196; *Chaos* ed D K Campbell (New York: American Institute of Physics) pp 153-72
- [4] Huberman B A and Lumer E 1990 *IEEE Trans. Circuits Systems* **37** 547  
Hogg T and Huberman B A 1991 *Controlling Chaos in Distributed Systems IEEE Trans. Systems, Man, Cyber.* special issue on distributed artificial intelligence, in press
- [5] Sinha S, Ramaswamy R and Rao J S 1990 *Physica* **D43** 118  
Sinha S 1991 *Phys. Lett.* **156A** 475
- [6] Ditto W L, Rauseo S N and Spano M L 1990 *Phys. Rev. Lett.* **65** 3211
- [7] Singer J, Wang Y-Z and Bau H H 1991 *Phys. Rev. Lett.* **66** 1123  
Vincent T L and Yu J 1991 *Dynamics Control* **1** 35
- [8] Azevedo A and Rezende S M 1991 *Phys. Rev. Lett.* **66** 1342
- [9] Braiman Y and Goldhirsch I 1991 *Phys. Rev. Lett.* **66** 2545
- [10] Romeiras F J, Ott E, Grebogi C and Dayawansa W P 1991 *Controlling Chaotic Dynamics Systems Proc. of the 1991 American Control Conference (IEEE)* in press
- [11] Hentschel H G E and Jiang Z 1991 Learning to control period-doubling bifurcations *Preprint*
- [12] Grebogi C, Ott E and Yorke J A 1982 *Phys. Rev. Lett.* **48** 1507; 1983 *Physica* **7D** 181
- [13] Kantz H and Grassberger P 1985 *Physica* **17D** 75
- [14] Nusse H E and Yorke J A 1989 *Physica* **36D** 137; 1991 *Ergod. Theor. Dyn. Syst.* **11** 189
- [15] Tél T 1990 *Directions in Chaos* vol 3, ed Bai-lin Hao (Singapore: World Scientific) pp 149-221
- [16] Grebogi C, Ott E and Yorke J A 1987 *Phys. Rev. A* **36** 3522
- [17] Cvitanović P 1988 *Phys. Rev. Lett.* **61** 2729
- [18] Tél T 1989 *J. Phys. A: Math. Gen.* **22** L691
- [19] Grebogi C, Ott E and Yorke J A 1983 *Phys. Rev. Lett.* **50** 935
- [20] Tél T 1987 *Phys. Rev. A* **36** 1502, 2507
- [21] Pianigiani G and Yorke J A 1979 *Trans. Am. Math. Soc.* **252** 351  
Ott E, Sauer T and Yorke J A 1989 *Phys. Rev. A* **39** 4212
- [22] Ditto W L *et al* 1989 *Phys. Rev. Lett.* **63** 923
- [23] Gorman M, Widmann P J and Robbins K A 1984 *Phys. Rev. Lett.* **52** 2241; 1986 *Physica* **D19** 255  
Widmann P J, Gorman M and Robbins K A 1989 *Physica* **D36** 157
- [24] Carroll T L, Pecora L M and Rachford F J 1987 *Phys. Rev. Lett.* **59** 28; 1989 *Phys. Rev. A* **40** 377, 4149; 1988 *J. Appl. Phys.* **64** 5396  
Carroll T L, Rachford F J and Pecora L M 1988 *Phys. Rev. B* **38** 2938  
Rödelsperger F, Weyrauch T and Benner H 1991 *Preprint*
- [25] Auerbach D *et al* 1987 *Phys. Rev. Lett.* **58** 2387  
Lathrop D P and Kostelich E J 1989 *Phys. Rev. A* **40** 4028
- [26] Smilansky U 1990 *Chaos and Quantum Physics* ed M-J Giannoni *et al* (New York: Elsevier) in press